

Monitoring of PV Inverters while Unintentional Islanding Using PMU

Szymon Henryk Barczeniewicz, Tomasz Lerch, and Andrzej Bień

Abstract—Unintentional islanding detection is one the mandatory criterion that must be met by PV inverters before connecting them into the grid. Acceptable time for inverter for islanding detection is less than 2 seconds. In this paper voltage parameters after islanding occurrence and before turning off the inverter are analyzed. In order to simulate islanding state and perform measurements the testing system was build. Three different commercial PV inverters were tested. Measured signals were used to calculate voltage envelope, phasor, frequency and ROCOF. Collected data proved to be helpful to compare different inverters.

Keywords—electrical disturbances; phasor measurement unit; power quality; PV inverters

I. INTRODUCTION

PHASOR technology consists of PMUs (Phasor Measurement Units), WAMS (Wide Area Measurement Systems), PDC (Phasor Data Concentrators) and IT applications. This technology was originally designed for transmission networks. In the highest voltage transmission networks, large powers are transmitted over long distances, and the issue of balancing a three-phase system is critical.

Balancing the system in a classic power grid, i.e. one where energy is generated in large power plants is a complex problem. Nevertheless, it is solved and mastered by grid operators in many countries around the world. In Figure 1a topology of classical system is presented.

According to the Energy Market Agency, in March 2021 the installed capacity of photovoltaics in Poland was almost 4.5 GW out of 51.7 GW of whole installed power. All renewable energy sources are 13.1 GW, which is approximately 25% of all types of electricity sources. In 2015, the installed capacity of photovoltaics was only 0.1 GW out of 37.3 GW of installed capacity.

Photovoltaic power plants, whether industrial or prosumer owned, are connected to a distribution network operating at lower voltages. Transmission powers and distances are small in comparison to transmission network powers. Due to the increase in the share of distributed energy sources (Fig. 1b), e.g. photovoltaic or wind, and the variability of loads, e.g. charging electric vehicles, air conditioning, three-phase distribution networks may be unbalanced. The level of disturbances in the distribution network, such as transients and harmonics, is therefore much higher than in the transmission network. One of

the responses to such phenomena is to build an appropriate monitoring system that will allow to react quickly and efficiently to dynamic changes in the system [1].

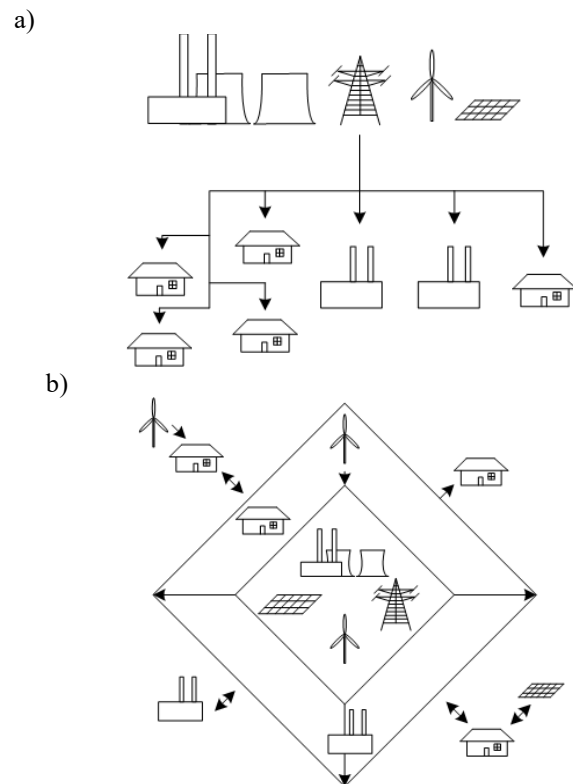


Fig. 1. a) Classical topology b) Smart Grid topology.

II. PHASOR MEASUREMENT

PMU measurement units [2,3] are recognized in the literature as the most important measurement devices in Smart Grid power systems [4]. PMU is usually a dedicated device, but also part or functionality within a large system.

A. Phasor Measurements Units

There are many different PMUs implementations, however IEEE Standard C37.118 [2] describes a generic model of PMU which consists of analog to digital converters (ADC), Global Positioning System (GPS) and phase-locked loop (PLL). The

Authors are with AGH University of Science and Technology, Poland (e-mail: {barczen, lerch, abien} @agh.edu.pl).



most important component of the device is capability of synchronizing its measurements with the universal time coordinated (UTC). This functionality is obtained with use of GPS or any other geopositioning system as well as other fiberoptic based synchronization methods.

Synchrophasors measured by PMU allow to obtain spatial awareness of the power system, visualize dynamic changes in the power system, mitigate or prevent failures or manage power flow.

In [1] the possibility of using PMU for detecting and monitoring selected electromagnetic disturbances was discussed, as well as the possibility of equipping PMU with additional functionalities such as: the availability of measuring synchronized waveforms of currents and voltages, measuring harmonic phasors and measuring residual signal which gives the possibility to calculate most of the power quality indicators.

B. Synchrophasors

Continuous time sinusoidal signal commonly used as a model of voltage and current is given with

$$x(t) = a(t) \cos(\omega_0 t + \varphi(t)), \quad (1)$$

where: $\omega_0 = 2\pi f_0$ is a nominal pulsation in rad/s, f_0 is a nominal frequency in Hz, $a(t)$ is time-varying amplitude and $\varphi(t)$ is a time-varying phase in radians. The phasor is defined as [2-5]

$$p(t) = \frac{a(t)}{\sqrt{2}} e^{j\varphi(t)}. \quad (2)$$

Figure 2 presents the convention of phasor representation shown in IEEE standard C37.118.1 [2].

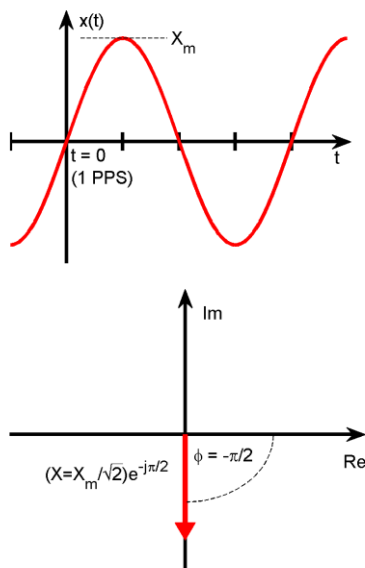


Fig. 2. Convention of phasor representation [1].

The instantaneous frequency f_{in} of (1) is the 1st order time derivative of cosine argument in (1):

$$f_{in}(t) = f_0 + \frac{1}{2\pi} \frac{d\varphi(t)}{dt} \quad (3)$$

and the rate of change of frequency (ROCOF) is the 2nd order time derivative of the cosine angle

$$ROCOF(t) = f \frac{1}{2\pi} \frac{d^2\varphi(t)}{dt^2} = \frac{df_{in}(t)}{dt} \quad (4)$$

III. UNINTENTIONAL ISLANDING

One of the applications of the phasor technology is islanding detection, especially in the context of photovoltaic farms and even prosumer micro-installations. Detection of islanding is one of the obligatory conditions that must be met by distributed generation systems. In the utility grid, an island forms when one or more distributed sources are disconnected from the utility grid but remain operational [6]. Such a situation may lead to accidents in teams carrying out repair work in the network. An additional problem may also be the exposure of the system to large energy fluctuations when the sources return to work with the system. A continuously working distributed source will not synchronize properly with the network when the network is back and running, which can lead to unwanted network protection reactions.

There are three groups of islanding detection methods: passive, active and communication based methods.

Passive methods are based on the monitoring of voltage parameters at the Point of Common Coupling (PCC) [7–11]. In these methods islanding is detected when observed parameters exceeds selected thresholds. Passive methods do not introduce disturbances into observed grid, they are simple and affordable which make them popular among inverters designers. Regrettably, these methods may not be able to detect islanding if the change of chosen parameters is too small, which makes the selection of appropriate thresholds crucial for their reliability. The range of observed parameters for which the islanding is not detected is called non-detection zone (NDZ). The oldest and most popular passive method is over/under voltage (UOV) and over/under frequency (UOF). Another very popular parameters used in passive methods is ROCOF and rate of change of voltage (ROCOV).

Active methods are based on monitoring the network's response to a deliberately introduced disturbance [11–14]. Thanks to this approach these methods can have a nearly zero NDZ, however they can affect power quality. There are many different active methods dedicated for specific distributed sources. Some of them are: phase shift methods, slip mode frequency shift methods, d-axis current injection methods [11] and q-axis current injection methods [12].

Communication methods use communication between a distributed source and the distribution network. They have zero NDZ. They are based on Power Line Communication (PLC) and Supervisory Control and Data Acquisition (SCADA) systems. However, such a solution may be too costly and it requires cooperation between the prosumer and the distribution network operator [15–18].

In [5] methods of island work detection with use of phasor technology were proposed. Such methods can be viewed as passive methods if one PMU is used for detection, or as hybrid methods if two PMUs are used. The method described in [5] is based on the observation of three basic parameters provided by the PMU: phasor, frequency and frequency variation called ROCOF. A particularly important parameter which is used to detect island operation is the frequency variation.

In this work the moment when the photovoltaic inverters are still in the operation before islanding is detected and the inverters are disconnected is emphasized.

IV. RESULTS

Laboratory setup consist of five main parts which are shown in the figure 3. PV phantom is the laboratory DC voltage source, with the programmable characteristic of the PV panel. EUT inverter is the tested power electronic unit which converts DC power to AC power with grid parameters. Power network was simulated using programmable grid simulator Chroma 61815, which allows precise voltage amplitude and frequency control. RLC load is based on programmable load that allows independent control of the load in each phase. Load can be regulated in 500 W intervals. Voltage during islanding operation is measured at the inverter terminals using data acquisition system cRIO-9024. Measurement system is a real time system with FPGA module which allows to measure different signal synchronously with multiple measurement modules. In this work voltage measurement units with 24 bit resolution were used. Chosen sampling frequency was 25 kHz.

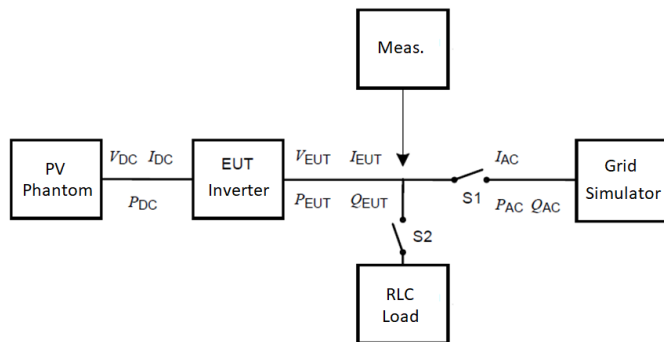


Fig. 3. Testing system for islanding [6].

Initiation of islanding in the presented system required an appropriate sequence of actions. At first S1 switch was switched on to synchronize inverter with the grid. In the next step, the PV phantom was programed for the inverter parameters and turned on. When the inverter has reached the maximum power point (MPP), the loads are turned on with switch S2. Then, by adjusting the operating point of the PV phantom, the inverter power was precisely equalized to equate it with the load power. When the power measured by the grid simulator was equal to zero (all the power generated by the inverter was consumed by the loads), the island operation was initiated by switching off the S1 switch. Before the island operation was initiated, a system recording the voltage waveform at the inverter terminals was activated.

Three one phase inverters of three different producers which are commercially available on the market where chosen for tests. Inverter 1 and 2 had 3 kW of nominal power and Inverter 3 had 4 kW nominal power. Such inverters are commonly found in the private prosumers PV installation in Poland, which makes them an interesting experiment object, that is fully grounded within current state of Polish electrical system.

It is worth noticing that according to IEEE standard 15471-2020 [6] the required time of disconnecting PV inverters should

not be longer than 2 seconds. All three inverters where staying in the operation for the time period between 1 s and 2 s long, after unintentional islanding state occurred, which means that time chosen for the analysis is within standard thresholds.

Measured signals where used to perform five different analysis: envelope of voltage, spectral analysis with additional THD calculation, discrete-time Fourier transform (DTFT) of voltage, phasor of voltage, frequency of voltage and ROCOF of voltage. There are a lot of different methods of phasor calculation. In this work phasor frequency and ROCOF were calculated with the use of the flat-top FIR filters [18-19] based on time signals acquired at 25 kHz sampling frequency and afterwards resampled to 800 Hz sampling frequency. Used method is fully compliant with the requirements of IEEE c37.118.1a standard [2].

A. Envelope

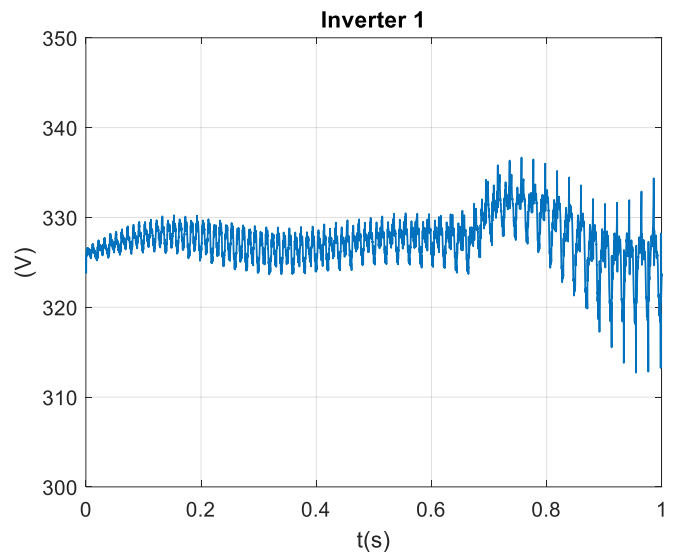


Fig. 4. Envelope of Inverter 1 instantaneous voltage value.

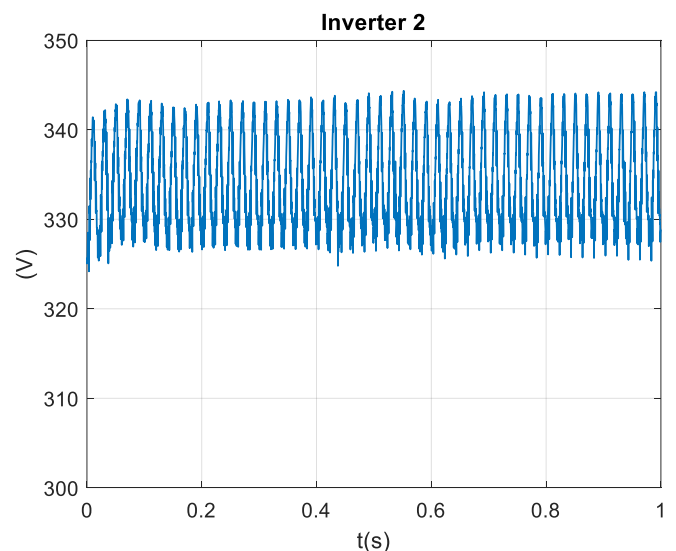


Fig. 5 Envelope of Inverter 2 instantaneous voltage value.

Envelope is calculated as an upper envelope of voltage as the magnitude of its analytical signal. Analytical signal was found by using Hilbert transform. Function hilbert() in Matlab returns complex helical sequence, sometimes called the

analytical signal. Hilbert function helps with calculating instantaneous attributes of times series, specifically amplitude and frequency information which are the most common parameters used for passive islanding detection method.

Figures 4, 5 and 6 present Inverters 1, 2 and 3 envelope of instantaneous voltage respectively.

We can observe that for Inverter 1 envelope starts to fluctuate significantly after 0.6 seconds. Similar performance was measured for Inverter 2, but without the fluctuations. For Inverter 3 we can observe higher fluctuations. Voltage changes from 305 V up to 348 V, however, observed changes are stable.

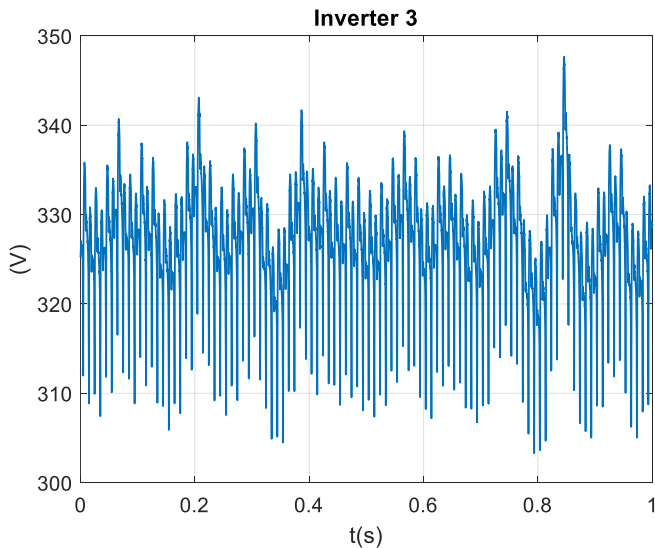


Fig. 6 Envelope of Inverter 3 instantaneous voltage value.

Comparing the performance of the three inverters in the context of envelope of voltage it is seen that Inverters 1 is possibly controlled in a different manner than the other two inverters. Inverter 2 and 3 are working in a relatively stable manner in contradiction to Inverter 1.

B. Spectrum analysis

Figure 7 presents DTFT of voltage for Inverter 1, 2 and 3. Frequency of voltage calculated for Inverter 2 and Inverter 3 is close to 50 Hz. Frequency for Inverter 1 is smaller than nominal frequency.

Figure 8 shows harmonics generated by inverters while unintentional islanding.

For every inverter odd harmonics were generated. Highest values of harmonics were registered for Inverter 3. In the figure 8 lowest values of harmonics are shown for Inverter 1. Lowest values may have been caused by the spectral leakage which is the result of unsynchronous sampling.

Table I presents THD in dBc of measured waveforms for tested inverters. The total harmonic distortion is determined from the nominal frequency and the first five harmonics using a modified periodogram of the length equal to the input signals length.

Inverter	THD [dBc]
1	-47.50
2	-45.44
3	-34.87

The highest THD was recorded for Inverter 3.

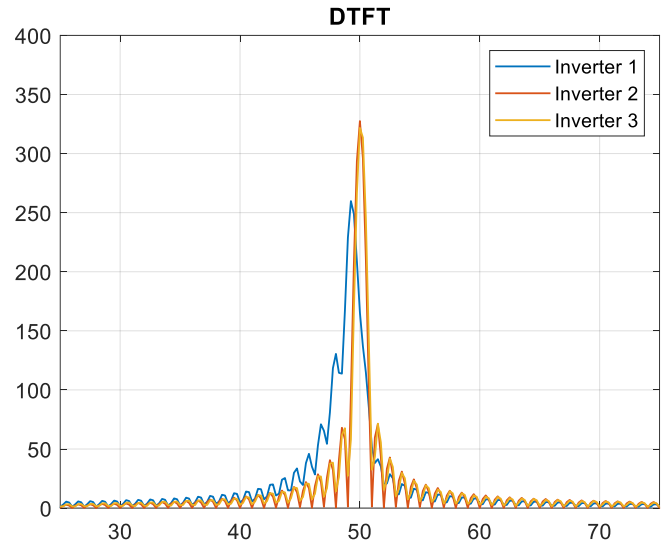


Fig. 7 DTFT of voltage of Inverter 1, 2 and 3.

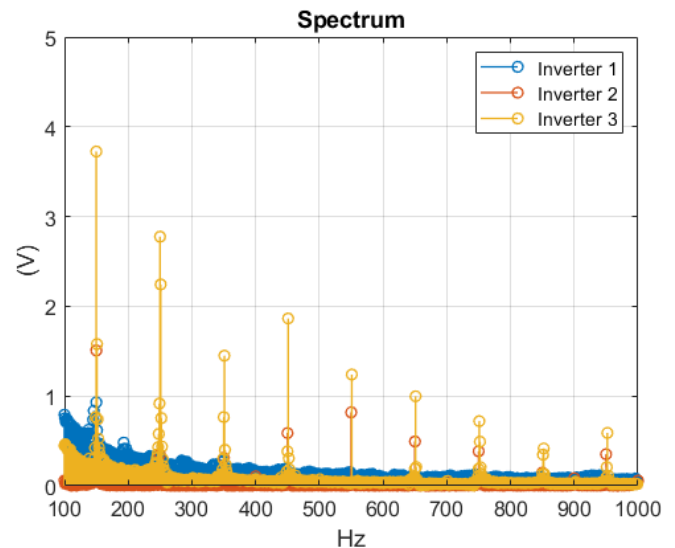


Fig. 8 Spectrum of voltage of Inverter 1, 2 and 3.

C. Phasor

Figure 9 shows phasors of voltage of Inverters 1, 2 and 3. The biggest fluctuations for phasor is observed for Inverter 3. Phasor of voltage is stable for Inverter 2.

Table II shows maximal, minimal and mean value of phasor for tested inverters.

Inverter	Max Phasor [V]	Min Phasor [V]	Mean Phasor [V]
1	332,0	325,8	327,8
2	328,2	325,4	327,8
3	332,2	319,5	326,4

Both smallest (319.5 V) and highest (332.2 V) value of voltage was registered for Inverter 3. The results are consistent with the results given by the spectral analysis as well as the THD calculation.

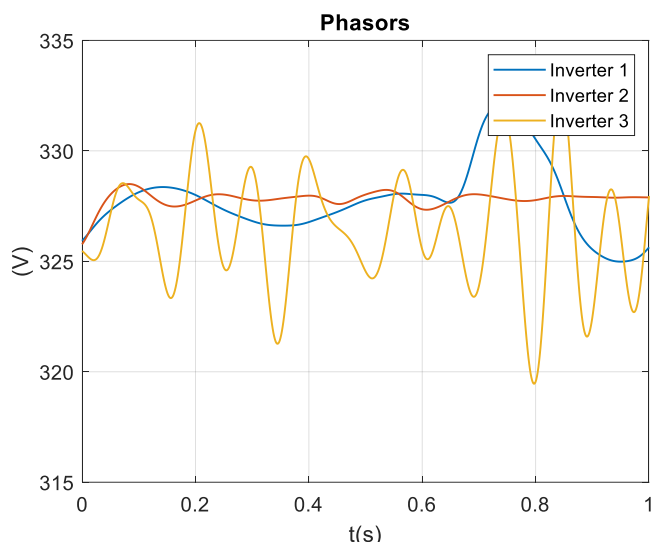


Fig. 9. Phasors of voltage of Inverter 1, 2 and 3.

D. Frequency

Figure 10 shows frequency of voltage of Inverters 1, 2 and 3. Inverters 1 frequency started to fall after the unintentional islanding state occurred. Frequency of Inverter 2 and Inverter 3 were stable and they fluctuated around constant value.

Table III shows maximal, minimal and mean value of frequency for tested inverters.

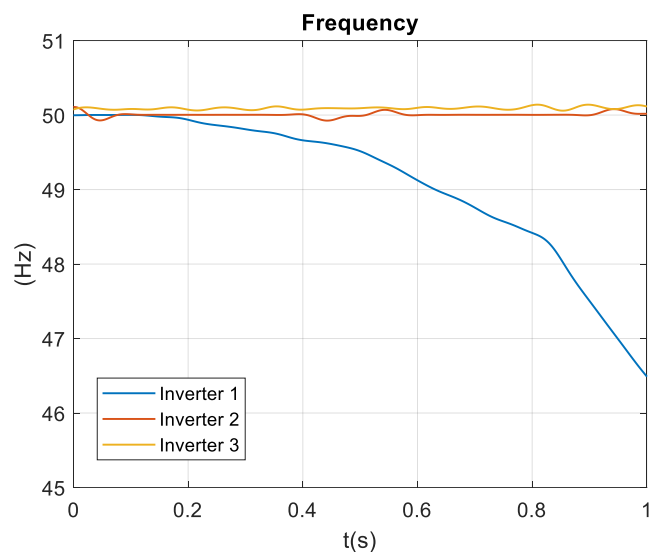


Fig. 10 Frequency of voltage of Inverter 1, 2 and 3.

TABLE III
RESULT FOR FREQUENCY

Inverter	Max Freq. [Hz]	Min Freq. [Hz]	Mean Freq. [Hz]
1	50.00	46.51	49.20
2	50.08	49.93	50.00
3	50.12	50.06	50.09

Smallest value of frequency was registered for Inverter 1 which was 46.51 Hz after steady fall from nominal frequency. Highest value 50.12 Hz was registered for Inverter 3. Frequency of Inverter 3 was stable but it was higher than nominal frequency which could have been caused by higher than power

generated by inverter than the power consumed by the load connected to the test system.

Comparison of inverters in the context of frequency shows that performance of Inverter 1 is significantly different from Inverter 2 and Inverter 3. This results are consistent with the results of the envelope based analysis.

E. ROCOF

Figure 11 shows ROCOF of voltage for Inverter 1, 2 and 3. ROCOF of Inverter 2 and 3 is close to 0 Hz/s. ROCOF of Inverter 1 is falling gradually. After 0.8 s ROCOF of Inverter 1 falls under -10 Hz/s.

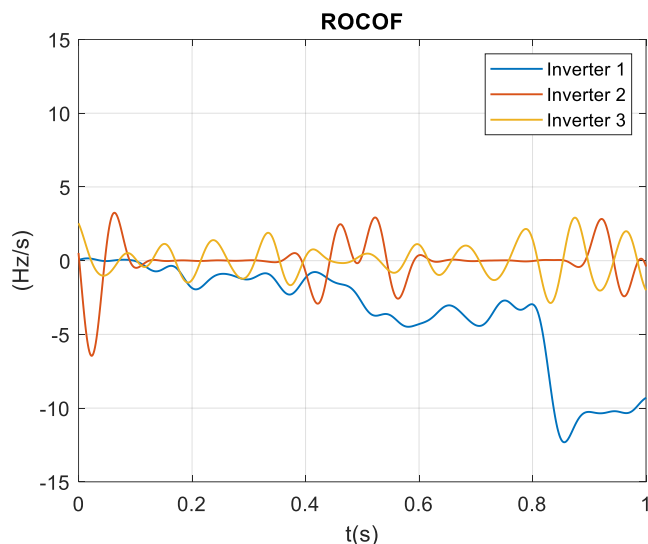


Fig. 11 ROCOF of voltage of Inverter 1, 2 and 3.

Table IV shows maximal, minimal and mean value of ROCOF for tested inverters.

TABLE IV
RESULT FOR ROCOF

Inverter	Max ROCOF [Hz/s]	Min ROCOF [Hz/s]	Mean ROCOF [Hz/s]
1	0.2	-12.3	-3.1
2	2.9	-6.4	-0.1
3	2.8	-2.8	0.0

Smallest value of ROCOF was registered for Inverter 1 which is -12.3 Hz/s. Highest value was registered for Inverter 2. Both Inverter 2 and 3 oscillated around 0 Hz/s which is consistent with the data obtained for frequency.

CONCLUSION

In this work the problem of monitoring of PV inverters while unintentional islanding using PMU was analyzed. In the paper the current situation on the photovoltaics market in Poland, especially in the context of small private prosumer installations, was reported.

Afterwards, the problem of unintentional islanding of PV inverters was explained and three different groups of methods of unintentional islanding: passive, active and communication based as well as the PMU based (both passive and hybrid of passive and communication) unintentional islanding detection methods were described and referenced.

PMU and the concept of synchrophasor was described using information obtained from both standards and the scientific literature.

Testing system for islanding was built using the requirements shown in the IEEE standard 15471-2020. Monitoring system based on the real time data acquisition system with FPGA module was built.

Three commercially available one phase PV inverters were tested. Test were performed for fully balanced system which means that the power generated by the inverter equaled the power consumed by the load. Analysis of voltage at PCC point were performed. Envelopes of voltage using Hilbert transform were calculated. Spectral analysis was performed using DTFT and DFT as well as a THD in dBc were calculated. Amplitude of Phasors, frequency and ROCOF of phasors were calculated using fully compliant FIR filters based on perfectly flat-top windows.

All three inverters that were tested in the presented work introduced different types of voltage distortions into the tested system (THD, voltage fluctuations). Inverters 1 frequency started to fall just after the unintentional islanding phenomenon. ROCOF as a derivative of frequency also started to change significantly for Inverter 1 just after unintentional islanding. Every inverters voltage phasors were fluctuating in a different manner. However, it is worth noticing that phasors values stayed within the nominal voltage ranges. In the case of Inverter 1 envelope of signal functionality which is focusing on information about amplitude and frequency proved to be reliable information in the context of monitoring of voltage while unintentional islanding.

Taking all these information into account it can be concluded, that as expected different PV inverters are controlled in a different manner. It is especially seen while comparing Inverter 1 to Inverter 2 and 3. This means that a proper monitoring system should be implemented to sustain the stability of prosumer or industrial PV plant owner network. Even though, the islanding should be detected and the inverter should be turned off, some of the distortions (voltage fluctuation, rapid frequency change) while unintentional islanding state could cause some problem i.e. for technological processes in industry (voltage controlled motors). Depending on the specific technological process a proper protection procedures should be implemented, remembering that PV inverters can still be in a operation even for 2 seconds according to PV inverters requirements introduced in the IEEE 15471-2020.

Summarizing, PMU is an equipment that can be successfully used for unintentional islanding detection as it is reported in the scientific literature, but it can also be used as a monitoring device while the islanding state itself.

The ability of monitoring multiple parameters especially the amplitude, frequency and ROCOF, as well as the possibility of calculating every power quality parameter after adding additional functionality (the availability of measuring synchronized waveforms of currents and voltages, measuring harmonic phasors and measuring residual signal) can help with the monitoring of PV farms both individual prosumers and bigger industrial PV farms.

REFERENCES

- [1] S. Barczeniewicz, A. Bień, K. Duda, „The use of PMU data for detecting and monitoring selected electromagnetic disturbances”, *International Journal of Electronics and Telecommunication*. 2020, <https://doi.org/10.24425/ijet.2020.134040>
- [2] IEEE Standard for Synchrophasor Measurements for Power Systems—Amendment 1: Modification of Selected Performance Requirements, IEEE Standard C37.118.1a, Apr. 2014.
- [3] *International Standard Synchrophasor for power systems – Measurements*, IEC/IEEE 60255-118-1, Edition 1.0, Dec. 2018.
- [4] G. A. Dileep, “Survey on smart grid technologies and applications”, *Renewable Energy*, vol. 146, pp. 2589-2625, 2020, <https://doi.org/10.1016/j.renene.2019.08.092>
- [5] S. Barczeniewicz, T. Lerch, A. Bień, K. Duda, “Laboratory Evaluation of a Phasor-Based Islanding Detection Method”. *Energies*. 2021; 14(7):1953. <https://doi.org/10.3390/en14071953>
- [6] IEEE 15471-2020 „Standard Conformance Test Procedures for Equipment Interconnecting Distributed Energy Resources with Electric Power Systems and Associated Interfaces”
- [7] S. Raza, H. Arof, H. Mokhlis, H. Mohamad, H. Azil Illias, “Passive islanding detection technique for synchronous generators based on performance ranking of different passive parameters”. *IET Gener. Transm. Distrib.* 2017, 11, 4175–4183, <https://doi.org/10.1049/iet-gtd.2016.0806>
- [8] Z. Lin, T. Xia, Y. Ye, Y. Zhang, L. Chen, Y. Liu, K. Tomsovic, T. Bilke, F. Wen, “Application of wide area measurement systems to islanding detection of bulk power systems.” *IEEE Trans. Power Syst.* 2013, 28, 2006–2015, <https://doi.org/10.1109/TPWRS.2013.2250531>
- [9] S.I. Jang, K.H. Kim, “An islanding detection method for distributed generations using voltage unbalance and total harmonic distortion of current.” *IEEE Trans. Power Deliv.* 2004, 19, 745–752, <https://doi.org/10.1109/TPWRD.2003.822964>
- [10] R. Teodorescu, M. Liserre, P. Rodriguez, “Grid Converters for Photovoltaic and Wind Power System” John Wiley & Sons, Ltd: Chichester, West Sussex, UK; 2011; pp. 93–96
- [11] S. Murugesan, M. Venkatarthiga, “Active Unintentional Islanding Detection Method for Multiple PMSG based DGs.” *IEEE Trans. Ind. Appl.* 2020, 56, 4700–4708, <https://doi.org/10.1109/TIA.2020.3001504>
- [12] S. Murugesan, V. Murali, “Hybrid Analyzing Technique Based Active Islanding Detection for Multiple DGs.” *IEEE Trans. Ind. Inform.* 2019, 15, 1311–1320, <https://doi.org/10.1109/TII.2018.2846025>
- [13] D. Sivadas, K. Vasudevan, “An Active Islanding Detection Strategy with Zero Non detection Zone for Operation in Single and Multiple Inverter Mode Using GPS Synchronized Pattern.” *IEEE Trans. Ind. Electron.* 2020, 67, 5554–5564, <https://doi.org/10.1109/TIE.2019.2931231>
- [14] M. Ropp, E. Aaker, K. Haigh, J. Sabbah, “Using power line carrier communication to prevent islanding”. *IEEE Photovolt. Spec. Conf.* 2002, 1675–1678, <https://doi.org/10.1109/PVSC.2000.916224>
- [15] X. Wilson, Z. Guibin, L. Chun, W. Wencong, W. Guangzhu, K. A Jacek, “Power line signaling based technique for anti-islanding protection of distributed generators-Part I: Scheme and analysis.”, *IEEE Trans. Power Deliv.* 2007, 22, 1758–1766, <https://doi.org/10.1109/TPWRD.2007.899618>
- [16] Z. Ye, R. Walling, L. Garces, R. Zhou, L. Li, T. Wang, “Study and Development of Anti-Islanding Control. for Grid-Connected Inverters”; Nat. Renew. Energy Lab.: Golden, CO, USA, May 2004, NREL/ SR-560-36243.
- [17] S. Katyara, A. Hashmani, B.S. Chowdhary, H.B. Musavi, A. Aleem, F.A. Chachar, M.A. Shah, “Wireless Networks for Voltage Stability Analysis and Anti-islanding Protection of Smart Grid System.” *Wirel. Pers. Commun.* 2020, 1–18, <https://doi.org/10.1007/s11277-020-07432-w>
- [18] K. Duda, T.P. Zieliński, S. Barczeniewicz, “Perfectly Flat-Top and Equiripple Flat-Top Cosine Windows”, *IEEE Trans. Instrum. Meas.* 2016, 65, 1558–1567, <https://doi.org/10.1109/TIM.2016.2534398>
- [19] K. Duda, T.P. Zieliński, “FIR Filters Compliant with the IEEE Standard for M Class PMU”. *Metrol. Meas. Syst.* 2016, 23, 623–636, <https://doi.org/10.1515/mms-2016-0055>